OPTOELECTRONICS AND ADVANCED MATERIALS – RAPID COMMUNICATIONS Vol. 3, No. 11, November 2009, p. 1161 - 1167

Synthesis, characterization and nonlinear optical studies of L-Leucinium Oxalate: a single crystal

M. ANBUCHEZHIYAN, S. PONNUSAMY[a*], C. MUTHAMIZHCHELVAN
Department of Physics, Valliammai Engineering College, Kattankulathur - 603 203, Kanchipuram (Dt.), India
[a]Centre for Material Science and Nano Devices, Department of Physics, SRM University, Kattankulathur - 603 203, Kanchipuram (Dt.), India

L-Leucinium Oxalate, (abbreviated as LLO) an organic nonlinear optical crystal was grown from aqueous solution. Transparent crystals of size 21mm × 5mm × 4mm were obtained. The grown crystals were characterized with single crystal X-Ray diffraction. The Powder X – Ray Diffractogram of the crystal has been recorded and the various planes of reflections are identified. The XRD studies confirm the crystalline nature of the complex. The chemical composition of LLO was determined by carbon, hydrogen and nitrogen (CHN) analysis. The qualitative analysis on the crystal has been carried by using Fourier Transform Infrared (FTIR) spectral measurements. The presence of hydrogen and carbon in the grown crystal was confirmed by using proton and carbon nuclear magnetic resonance (NMR) spectral analyses. Optical behavior of the crystal was studied using UV – Visible spectroscopy. The mechanical strength of the grown crystals was found by using Vickers micro hardness test. The dielectric behavior of the crystal was determined at room temperature in the frequency range of 70 Hz to 5 MHz. The thermal stability and decomposition of the crystal were studied by thermogravimetric analysis (TGA) and Differential Scanning Calorimetry (DSC). The nonlinear optical property of the crystal was tested by Nd:YAG laser source.

(Received April 24, 2009; accepted October 29, 2009)

Keywords: Growth from solution, NLO materials, X-ray diffraction, Spectral studies, Thermal studies

1. Introduction

In the past three decades, nonlinear optical (NLO) materials have attracted much attention because of their potential applications in the field of optical communications, high-speed information processing, optical data storage and in emerging optoelectronics technology [1,2]. Recently there have been extensive efforts to develop new organic, inorganic and semi organic NLO crystals. There has been growing interest in organic crystals because of their possible application in the field of NLO [3]. The organic materials offer the advantage of higher NLO activity and faster response times. The key factor for material selection depend not only the laser conditions but also on the physical properties of the crystals. The crystal structures of amino acids and their complexes have provided interesting information about aggregation, and the effect of other molecules on their interaction and molecular properties. Amino acids are bifunctional organic molecules that contain both a carboxylic group as well as an amino group. In solid state amino acid contains protonated amino group and de-protonated carboxylic group. This dipolar exhibits peculiar physical and chemical properties. So the efforts have been made on the amino acid mixed crystal in order to make them suitable for device applications. Some complexes of amino acids with organic or inorganic acids exhibit NLO properties [4 - 6]. This interest has been fuelled by the possibility of using them in the technological devices. Some oxalates are reported to be Second Harmonic Generation (SHG) active and also such behavior of L-Alaninium oxalate [7] and Glycinium oxalate [8] was recently reported. Hence it may be useful to synthesize the amino acid complexes with oxalic acid and study their properties. Attempt to crystallize such complexes are under progress in our laboratory and L-Leucinium Oxalate (LLO) was successfully grown. The structure of LLO was elucidated by Rajagopal et al. [9]. LLO is one such organic crystal that belongs to the Leucine-complex family. In the present study, bulk single crystals of LLO were grown and hence attempts are made to characterize the grown crystal by single crystal XRD, powdered XRD, CHN, FTIR, FT NMR, UV-Visible, micro hardness, thermal analysis and dielectric studies. The SHG studies of the LLO was also studied using Nd:YAG Q- switched laser.

2. Experimental procedure

2.1 Synthesis and crystal growth

The LLO crystal was synthesized by taking Leucine ($C_6H_{13}NO_2$) and oxalic acid ($C_2H_2O_4$) in the appropriate ratio. The calculated amounts of Leucine and oxalic acid were thoroughly dissolved in double distilled water using a temperature controlled magnetic stirrer. The solution was stirred well and slightly warmed using magnetic stirrer and filtered using filter paper and transferred to Petri dish. The prepared solution was allowed to evaporate at room temperature, which yield the salt of LLO. The purity of the synthesized salt was further improved by re-crystallization process. Saturated solution of LLO taken in a beaker of

100 ml capacity was optimally closed using a perforated thin polyethylene sheet and was kept in a constant temperature bath equipped with EUROTHERM temperature controller of accuracy ± 0.01 K. The temperature was maintained at 35°C and solutions were allowed to evaporate. Transparent crystals of size 21 × 5 × 4mm^3 were grown in a period of 45 days. The grown crystal of LLO is shown in Fig. 1.

Fig. 1. As grown crystal of LLO.

2.2 Characterization

In order to collect X-Ray diffraction data of LLO crystal, single crystal XRD studies have been carried out using BRUKER AXS KAPPA APEX (II) CCD diffractometer with Mo Kα (λ= 0.710693 Å) radiation. The unit cell dimensions were determined. The powdered sample of single crystal LLO was subjected to powder X-ray diffraction studies with a high resolution PANalytical X'pert PRO diffractometer. Finely ground powder of the crystals were subjected to intense X-rays of wavelength λ = 1.5406 Å with a scan speed of 0.04° per second. Intensities for the diffractions peaks were recorded over the range of (2θ) 20º - 85º. CHN analyses were carried out using Vario EL III Elemental analyzer. To determine the optical absorbance range and hence to know the suitability of LLO single crystals for optical applications, the UV – Visible absorbance spectrum has been recorded using a Perkin Elmer Lambda 25 spectrophotometer in the range 200 – 800 nm covering the entire UV and Visible region. The FTIR spectra of the samples were recorded in the KBr phase in the frequency region of 400 cm^{-1} – 4000 cm^{-1} using Perkin Elmer FTIR Spectrometer. In the present investigation, the ^{1}H and ^{13}C NMR spectrum of the grown crystal has been recorded with a Bruker Avance III 500 MHz spectrometer with D_2O as solvent. The dielectric constant and the dielectric loss of the LLO sample were studied at room temperature using HIOKI 3532-50 LCR HITESTER instrument from 70 Hz to 5 MHz. LLO crystals was subjected to static indentation test at room temperature using SHIMADZU hardness tester fitted with Vickers diamond pyramidal indenter. The thermo gravimetric analysis (TGA) and differential thermal analysis (DTA) of the crystal were carried out using the instrument NETSZCH STA 409 C/CD. The TGA-DTA curve of LLO was recorded between 25ºC and 1200ºC at a heating rate of 10K/min in the nitrogen atmosphere. Alumina was used as the reference. The differential scanning calorimetry (DSC) studies have also been recorded using NETZSCH DSC 204 between the temperature range 25ºC to 300ºC at a heating rate of 10K/min. Kurtz and Perry powder method was employed to check the SHG test of LLO crystal. The crystal was eliminated using spectra physics quanta ray model LAB-170-10 Nd;YAG Q-switched laser system operated at repetition rate of 10Hz with maximum pulse energy of 850mJ. The SHG output of green light (532nm) was finally detected by the power meter EPM 2000 TOP Assy, Grey with J-50MB-YAG-Energy Max Sensor Head.

3. Results and discussion

3.1 Single crystal and powder X-ray diffraction analysis

Well shaped, transparent, single crystals of LLO were selected and it was subjected to single crystal X-ray diffraction study at room temperature. Intensity data were collected up and final unit cell parameters were based on all reflections. From the single crystal analysis it was observed that the crystal belongs to triclinic crystal system having non-centrosymmetry with P1 space group. Lattice parameters have been determined as: a = 5.66Å, b = 9.79Å, c = 9.89Å, α = 87.45º, β = 99.54º, γ = 100.27º and the volume of the unit cells is found to be 531Å^3. These values are in good agreement with the reported values [9]. The molecular structure of the grown LLO crystals is as shown in Fig. 2.

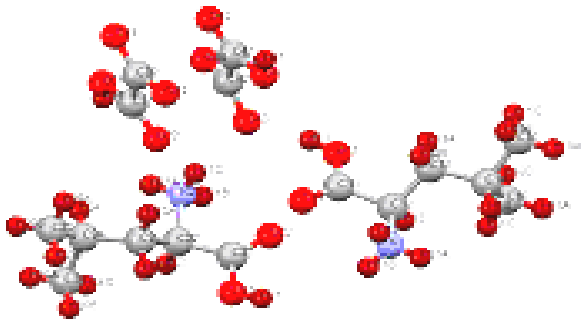

Fig. 2. Molecular structure of LLO crystal.

X-Ray powder diffraction was used for the identification of the synthesized LLO crystal. Efforts were made to record the powder XRD pattern of the L-Leucinium oxalate crystal and index them. The indexed powder XRD pattern of the grown LLO crystal is shown in Fig. 3. The XRD powder pattern has been indexed using CELREF programs and the lattice parameters are evaluated as: a = 5.6740Å b= 9.8055 Å c= 9.9063Å, α = 87.35º, β = 99.62º and γ =100.34º. The volume of the unit cell is 534.327Å^3. The calculated lattice parameters from the powder XRD analysis are in good agreement with the literature reported [9].

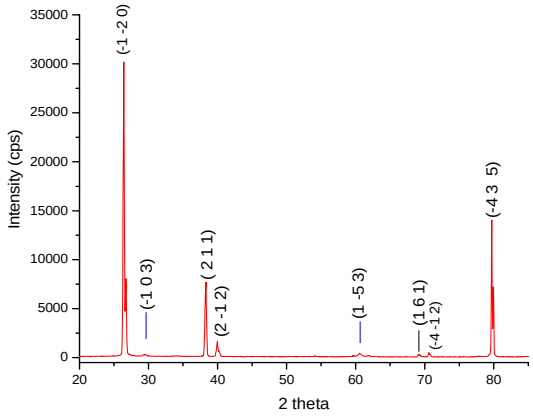

Fig. 3. Powder XRD pattern of LLO.

3.2 CHN analysis

The grown crystals of LLO were then characterized by CHN test. Results obtained from CHN analysis are compared with the theoretical value of carbon, hydrogen and nitrogen present in LLO crystal and are given in Table 1. Both are consistent with each other indicating the formation of the crystal.

Table 1. Chemical analysis of LLO crystal (molecular weight = 221.208).

Element	Composition (%)	
	Theoretical	Measured
Carbon	43.436	43.42
Hydrogen	6.834	6.90
Nitrogen	6.33	6.323

3.3 FTIR spectral analysis

Infrared Spectroscopy is used to identify the functional groups of the synthesized compounds. The recorded FTIR spectrum of LLO is shown in the Fig. 4. The complete vibration analyses of the observed bands are presented in the Table 2. All the spectral data are compared with the standard spectrum of these functional groups [10, 11]. From the FTIR, bands at 1394 and 1453 cm^{-1} are associated to symmetric bending and asymmetric bending of CH_3. The bands observed at 1568 and 1621cm^{-1} are associated to stretching vibration of CO_2^- and the bending vibration of NH_3^+. This shows the zwitterionic nature of grown compound. The 900 -1100 cm^{-1} spectral region is characterized by bands associated to several CC and CN stretching vibrations. The strong band attributed at 1121 cm^{-1} is assigned as rocking of NH_3^+unit and as well as at 1182 cm^{-1}. The strong band at 1246 cm^{-1} is torsion of CH_2. Bands due to the stretching vibrations of methylene, methane and ammonium groups are expected to be observed in these high wave number regions 2800-3100 cm^{-1}. However, as it is well known, the bands associated to the stretching vibrations of the NH_3^+ group's present broad band at 3080 cm^{-1} in the FTIR spectrum. The OH stretching vibration is present, a large band centered at 3380 cm^{-1}. Skeleton is observed in the crystal structure of L-Leucine almost all the crystal of L-Leucine with organic and inorganic acids except the present work LLO and L-Leucine Leucinium Picrate [12]. From this spectroscopic analysis, the presence of all the fundamental functional groups of the grown sample was confirmed qualitatively.

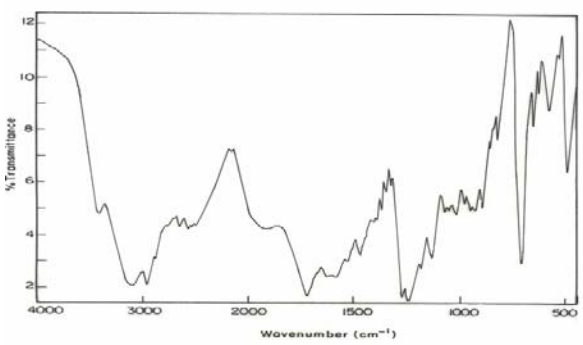

Fig. 4. FTIR spectrum of grown crystal LLO.

Table 2. Vibrational assignments of the grown LLO crystal.

FTIR of present work (cm^{-1})	Vibrational assignment
3380 s	ν OH
3080 vs	ν NH_3^+
2960 vs	ν –CH of –C-$(CH_3)_2$
2870 vs	$\nu_{asymmetric}$ (CH_3)
2630 s	$\nu_{symmetric}$ CH $(C(NH_3)^+)$
2480 s	$\nu_{symmetric}$ CH
1720 vs	ν C=O
1621 vs	δ (NH_3^+)
1568 vs	ν (CO_2^-)
1454 s	$\delta_{asymmetric}$ (CH_3)
1394 s	$\delta_{symmetric}$ (CH_3)
1371 s	C-C-H in plane deformation
1364 s	NH_3^+ twisting
1333 m	δ (CH)
1303 m	δ C-O-H
1273 s	ν C-O
1246 s	τ (CH_2)
1182 vs	r (NH_3^+)
1121 vs	r (NH_3^+)
1061 s	ν (CN)
1035 s	ν (CN)
1001 s	ν (C-C)
963 m	ν (C-C)
932 s	ν (C-C)
917 s	ν (C-C)
888 s	r (CH_3)
827 w	γ (CO_2^-)
798 w	δ (CO_2^-)
709 vs	δ (CO_2^-)
634 w	w (CO_2^-)
604 vw	w (CO_2^-)
560 w	r (CO_2^-)
507 vw	r (CO_2^-)
483 m	r (CO_2^-)

s-strong; vs- very strong; m-medium; w-weak; vw-very weak
ν, stretching; γ, Out-of- plane vibration; δ, bending; τ, torsion; w, wagging; r, rocking.

3.4 FT NMR spectral analysis

FT NMR spectroscopy is used to determine the molecular structure based on the chemical environment of the magnetic nuclei like ^{1}H, ^{13}C, ^{31}P, etc., even at low concentrations. This is one of the most powerful nondestructive techniques in elucidating the molecular structure of the biological and chemical compounds. The FT NMR spectrum of the title crystal is presented in Fig. 5 (a) and (b) respectively and the chemical shifts are represented in δ ppm. An intense singlet observed at 4.691δ (ppm) in the Proton NMR spectrum is due to the presence of undeutrated water and moisture. The signals due to N-H and COOH protons do not show up because of fast deutrium exchange taking place in these two groups, with D_2O being used as the solvent [7,13]. CH proton of the C_2 carbon of leucine appears as a multiplet at 3.9 ppm. CH_2 protons of the C_3 carbon and CH proton of the C_4 carbon of leucine appear as multiplet in the range of 1.6 and 1.8 ppm. Six protons of CH_3 groups appear as a doublet at 0.8 ppm. In the Carbon NMR, the second carbon atom (C_2) of the leucine moiety gives a peak at 51.65 ppm. C_3 carbon of the leucine appears at 38.94 ppm. C_4 carbon of the leucine gives absorption at 23.93 ppm. Two carbon atoms of the methyl groups of the leucine moiety appear at 21.61 and 20.84 ppm. Carbon of the carboxylate anions of oxalic acid moiety appears at 164.61 ppm. Carbon of the COOH groups of the leucine and oxalic acid moieties appear at 173.08 ppm. Thus, the molecular structure of LLO is confirmed by ^{1}H and ^{13}C NMR spectral studies.

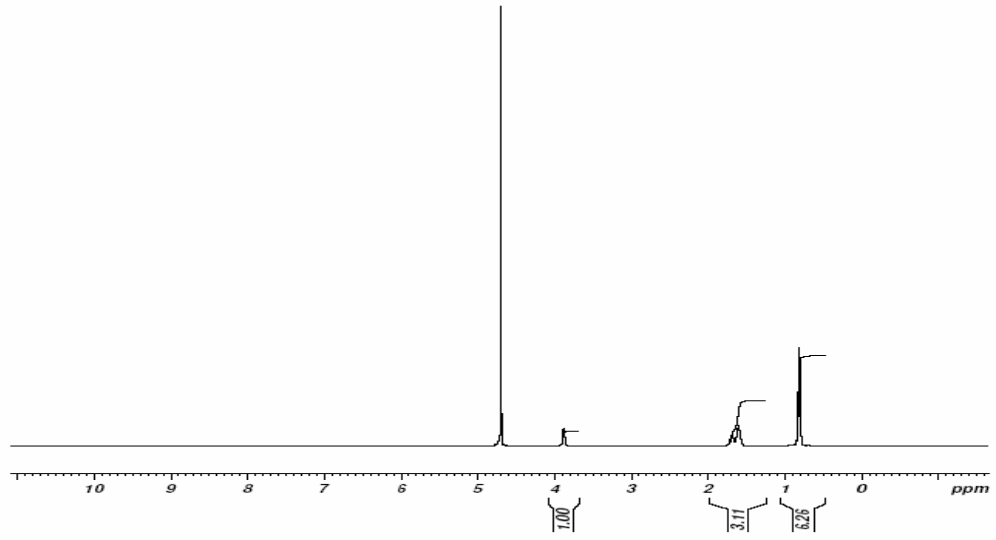

(a)

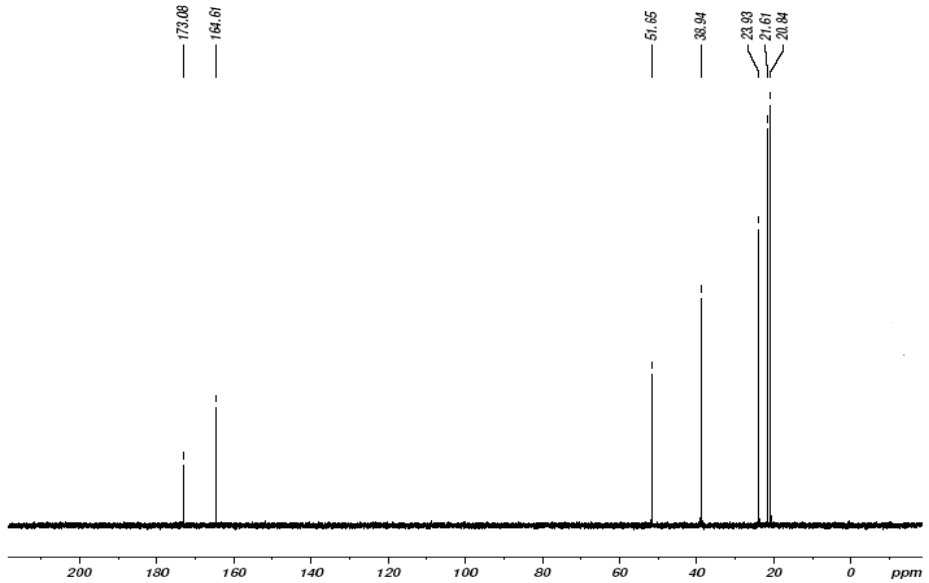

(b)

Fig. 5. (a). HNMR spectrum of LLO; (b). CNMR spectrum of LLO.

3.5 UV-Vis analysis

UV-Visible spectrum gives information about the structure of the molecules because the absorption of UV and Visible light involves promotion of the electron in the π orbital to the high energy π* orbital. The recorded spectra are shown in the Fig. 6. In the present study, the optical behaviour was examined between 200 to 800 nm. The absence of absorption in the region between 219 and 800 nm in the UV-Vis spectrum showed that this crystal is good enough for the second harmonic generation of Nd-YAG laser of wavelength (1064 nm). It is a requirement for NLO materials having nonlinear optical applications [14].

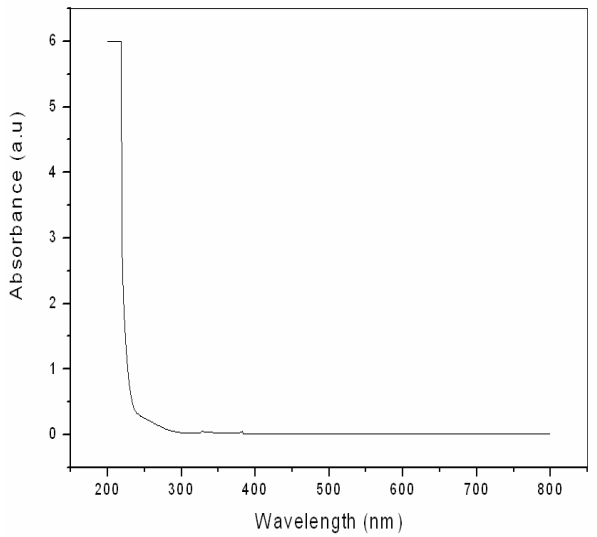

Fig. 6. UV-VIS absorbance spectrum of LLO.

3.6 Powdered SHG studies

The second harmonic generation conversion efficiency of LLO crystal was measured by Kurtz and Perry method [15]. The crystals was grounded in to a homogenous powder of particles and densely packed between two transparent glass slides. A Q-switched Nd:YAG laser emitting a fundamental wavelength of 1064 nm pulse width of 8 ns was allowed to strike on the sample cell normally. 532 nm second harmonic generation output beam pulse energy of 3.6 mJ was obtained with 0.5 J of an input of 1064 nm fundamental pulse energy at a repetition rate of 10 Hz. Thus the SHG was confirmed by the emission of green light.

3.7 Vickers microhardness measurements

Hardness of the crystal carries information about the strength, molecular binding, yield strength and elastic constants of the materials [16]. In the present study, micro hardness measurements were carried out on LLO single crystals. Vickers microhardness number was then evaluated from the relation:

$$H_v = 1.8544\ P/\ d^2 \quad (kg/mm^2)$$

where, 'H_v' is the Vickers microhardness number, 'P' is the applied load and'd' is the diagonal length of the indentation impression.

To evaluate the Vickers hardness, several indentations were made on the face of the crystal. The diagonal length of the indentations was measured using a micrometer eyepiece. Dependence of the microhardness on the load for LLO crystal has been evaluated. Load of different magnitude (25 and 50 g) were applied on the LLO crystal for the fixed interval of time. Hardness is found to decreases as the load is increases. The measurement of Vickers microhardness values are as shown in a Table 3. The load above 50g develops multiple cracks were initiated on the crystal surface due to the release of internal stresses generated locally by indentation. So, it may suggest for the NLO applications below 50g of applied load. This implies that LLO single crystal is a good engineering material for device fabrications.

Table 3. Hardness measurement.

Load (gm)	L1 (micro metre)	L2 (micro metre)	H_V (kg/mm^2)
25	28.13	30.36	54.1
50	46.96	51.29	38.4

3.8 Dielectric studies

The dielectric constant and the dielectric loss of the LLO sample were studied at room temperature using HIOKI 3532-50 LCR HITESTER 70 Hz to 5 MHz. The dielectric constant and the dielectric loss were measured with varying frequency, for a fixed applied voltage. Figs. 7 and 8 show the variation of the dielectric constant and the dielectric loss as a function of log frequency at room temperature. The value of dielectric constant of the LLO crystal is calculated using the formula

$$\varepsilon_r = Cd/\varepsilon_0 A$$

where ε_0 is the permittivity of free space = 8.854×10^{-12} F/m, C is the capacitance of the LLO crystal in Farad, d is the thickness of the specimen in m; A is the area of the specimen in m^2. The output of LCZ Bridge at room temperature was measured. The values of dielectric constant at room temperature were calculated. The dielectric constant ε_r of LLO shows the variation with frequency as shown in Fig 7. Dielectric constant is found to decrease with increasing frequency, at room temperature. The high value of dielectric constant at lower frequencies may be due to the presence of all the four polarization namely, space charge, orientational, ionic and electronic polarization and its low value at higher frequencies may be due to the loss of significance of these polarization gradually [17]. From the Fig. 8 shows the variation of dielectric loss with applied frequency and it

was observed that the dielectric loss was reduced at higher frequencies. The characteristic of low dielectric loss at higher frequency ranges shows that the LLO crystal possesses good quality with lesser defect which is important for NLO applications [18].

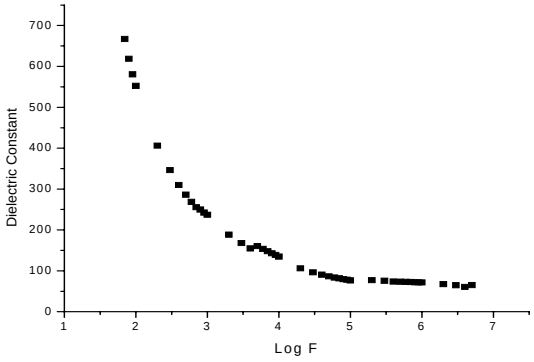

Fig. 7. Log F versus dielectric constant of LLO at room temperature.

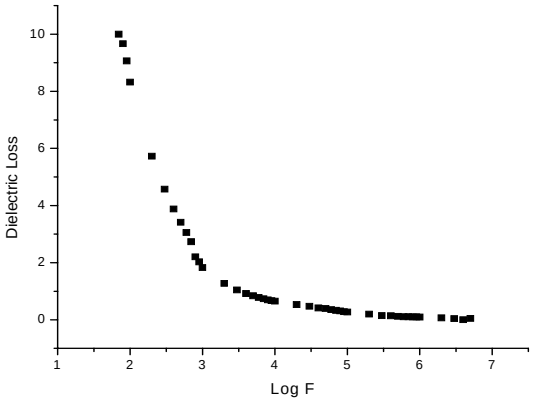

Fig. 8. Log F versus dielectric loss of LLO.

3.9 Thermal analysis

TGA-DTA and DSC have been carried out for the grown crystals. The TGA-DTA and DSC curves are shown in Figs. 9 and 10, respectively. 29.36 mg of the sample was taken to carry out the experiment. From the TGA curve, two stages of decomposition have been identified. First stage decomposition in the temperature range 203 to 222ºC with the mass change of 40% and second stage goes up to 353ºC for the mass loss of 60%. It is observed from the TGA curve, that the compound undergo an irreversible endothermic transition occurs at 203.4ºC which corresponds to the beginning of the decomposition. In the first stage decomposition CO_2, CO, and H_2O are evolved probably by the decomposition of oxalic acid. The weight loss corresponds to the evolving volatile substances. The second stage decomposition starts from 222ºC and goes up to 353ºC. The probable volatile substances are CO_2, NH_3 and C_5 alkene. The materials melt at 160ºC (as observed by VEEGO melting point apparatus) and the molten liquid is stable up to 203ºC. The melting point of the material as seen from the DSC curve is 162ºC. LLO crystals is stable up to 203ºC.There is no phase transition till the material melts and this enhances the temperature range for the utility of the crystal for NLO applications

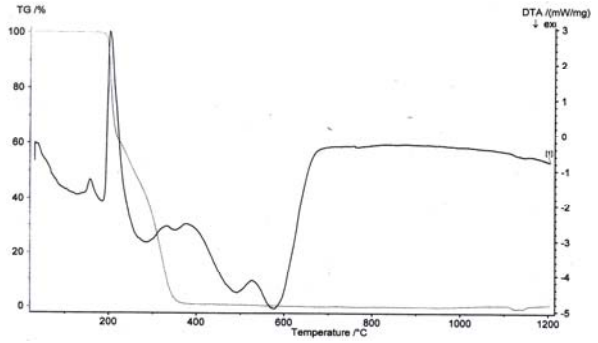

Fig. 9. TGA-DTA curve of LLO.

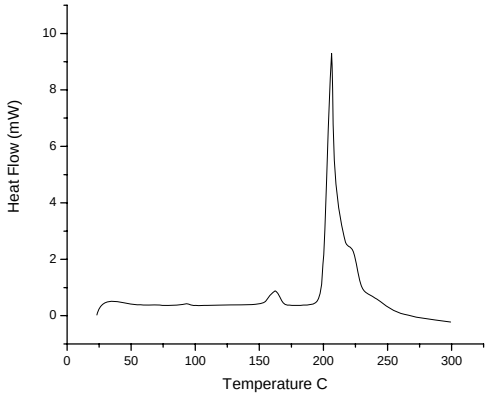

Fig. 10. DSC curve of LLO.

4. Conclusions

Single crystals of size up to 21 × 5 × 4mm^3 were obtained using solution growth technique. The grown crystals were characterized by single crystal and powder XRD to deduce the unit cell parameters. These lattice parameters are close agreement with the reported values. Vibrational frequencies were identified and assigned from FTIR spectral analysis, which confirms the presence of functional groups of the LLO crystals. Our NMR results confirm the crystal structure of LLO. The UV-Visible spectrum of LLO showed that the crystal is transparent in the range of 219 - 800 nm. Vickers hardness values measured gives its mechanical strength. The optical characterization of these single crystals shows the second harmonic generation. The dielectric constant and dielectric loss of the crystal were studied for a wide range of frequencies. It suggested that the grown crystal is free

from defects. From the thermogram, it is concluded that the compound undergoes no phase transition and is stable up to 203ºC.

Acknowledgements

The authors express their sincere thanks to the Head, SAIF, IIT Chennai; The Head ICP section CECRI Karaikudi for characterizations. The authors also thanks to Mr. Narayanan IIT Chennai, Dr. Basheer Ahamed Crescent Engineering College (SHG studies) and Dr. Chaarles C. Kanagam, Valliammai Engineering College for useful discussions

References

[1] David F. Eaton, Science **253,** 281 **(**1991).
[2] V. G. Dmitriev, G. G. Gurzadyan, D. N. Nikgosyan, Hand book of nonlinear optial crystals, 2nd ed., Springer, New York, 1997.
[3] D. J. Williams, Nonlinear Properties of Organic and Polymeric Materials; ACS Symp. Ser. 233, 1983.
[4] S. B. Monaco, L. E. Davis, S. P. Velsko, F. T. Wang, D. Eimerl, A. Zalkin, J. Cryst. Growth **85**, 252 (1987).
[5] D. Eimerl, S. P. Velsko, L. E. Davis, F. T. Wang, G. Loiacono, G. Kennedy, IEEE J. Quantum Electron. **25**, 179 (1989).
[6] H. L. Bhat, Bult. Mater. Sci. **17,** 1233 (1994).
[7] S. Dhanuskodi, K.Vasantha, Cryst. Res. Technol**. 39**, 259 (2004).
[8] P. Mythili, T. Kanagasekaran, R. Gopalakrishnan, Mater.Lett. **62,** 185 (2008).
[9] K. Rajagopal, R. V. Krishnakumar, M. Subha Nandhini, R. Malthi, S. S. Rajan, S. Natarajan, Acta Cryst. E **59,** o878 (2003).
[10] P. F. Facanha Filho, P.T.C. Freire, K. C.V.Lima, J. Mendes Filho, F. E. A. Melo, P. S. Pizani, Brazilian journal of physics **38**, 131 (2008).
[11] R. Silverstein, Webster, Spectroscopic identification of Organic compounds sixth ed., Willey, New York, 1998.
[12] Jan Janczak, Genivaldo Julio Perpetuo, Acta cryst. C **63**, o117 (2007).
[13] P. Y. Bruice, Organic Chemistry, Pearson Education (Singapore) Pte.Ltd., First Indian Reprint, New Delhi, 2002.
[14] N. Vijayan, R. Ramesh Babu, R. Gopalakrishnan, P. Ramasamy, W. T. A. Harrison, J. Cryst. Growth **262,** 490 (2004).
[15] S. K. Kurtz, T. T. Perry, J. Appl. Phys. **39**, 3798 (1968).
[16] B. Ducourant, R. Fourcade, G. Mascherpa, Rev.Chim.Miner. **20,** 314 (1983).
[17] S. A. Martin Britto, S. Natarajan, Opt. Commun. **281,** 457 (2008).
[18] C. Balarew, R. Duhlew, J. Solid State Chem. **55**, 1 (1984).

*Corresponding author: suruponnus@gmail.com